

Model for Increased Energy Deposition in a γ -Irradiated Nylon via a Nickel Microphase

R. P. Kusy*

Department of Metallurgical Engineering, Drexel University,
Philadelphia, Pennsylvania 19104. Received November 24, 1975

ABSTRACT: A model is developed to explain the increased energy deposition which occurs in certain multiphase systems having large differences in electron densities after exposure to high-energy electromagnetic radiation. The composite geometry selected favors the escape of Compton recoil electrons from the high electron density phase into the low electron density medium. There the more numerous Coulombic interactions increase the chemical changes for small volume fractions of the high electron density phase, although the production and reabsorption of secondary electrons remain proportional to the electron densities of each phase. A comparison of $G(-\text{units})_{\text{total}}$ derived from the theoretical model agreed with the experimental results obtained previously from cryoscopic measurements. The limitations and general applicability of the model are discussed.

I. Introduction

In earlier work¹ electrically conductive cylinders (1.5 cm diameter \times 2 cm high) were formed by compacting particles of nickel (3–7 μm , Ni-123, International Nickel Co.) with, on the average, much larger particles of nylon-66 (5–100 μm , Zytel 101, du Pont de Nemours Co.) for 10 min at room temperature under 1000 kg/cm². To attain sufficient mechanical strength, the “green” compacts were irradiated with Co⁶⁰ γ rays and post-irradiation heat treated at 525 K. In spite of a constant irradiation dose, the percent gel was found to increase substantially with additions of nickel, suggesting that an increased radiation deposition had occurred from the interaction of the nylon with the higher electron density phase. To substantiate these results, cryoscopic measurements were made at a programmed heating rate of 20 K/min on a du Pont Differential Thermal Analyzer (DTA) and the $G(-\text{units})$ chemically changed were determined by the depression of the melting point, or

$$G(-\text{units}) = [(1 - X)N_A \times 10^2]/D(6 \times 10^{19})M$$

in which

$$X = \exp\left[-\left(\frac{\Delta H}{R}\right)\left(\frac{1}{T} - \frac{1}{T_0}\right)\right] \quad (\text{ref } 2)$$

The significance of these expressions has been detailed elsewhere.^{1,3} For the case in which the volume fraction of nickel equalled zero, results showed that the cryoscopic measurements of $G(-\text{units}) = 7.5\text{--}9$ were in good agreement with Zimmerman,⁴ $G(-\text{free radicals}) = 5.8$. Moreover, the value for $G(-\text{unit})_{\text{total}}$ clearly increased (56–73%) with the addition of 15% nickel by volume (Figure 1).

To explain this phenomenon, a model is proposed which utilizes the “segregated” distribution¹⁸ described previously (cf. Figure 2 of ref 5). Here the polymeric material, P, and metal, M, emit secondary electrons in proportion to their electron densities. The geometry is such that the probability of secondary electron escape from the pointlike sources, M, and into the low density medium is high. There, these additional recoil electrons create Coulombic interactions in P above the normal level found. Although the termination of these recoil electrons is proportional to the electron density, the increased production of primary free radicals from the Coulombic interactions increases the G value of the polymer matrix.

II. Model

(1) Assumptions. Three assumptions must be valid for the segregated particulate distribution to increase the G value of

the polymer matrix: (i) the particles of material M must be sufficiently small, i.e., approximate point sources, so that the primary Compton scattering events can escape initially into the lower density medium; (ii) the resultant energy profile in P must be homogeneous, that is to say, each electron which emanates from an M particle must have a high probability of passing through and providing Coulombic interactions over many polymeric diameters; and (iii) the emission from individual point sources around particles of P is not absorbed by the cross section of immediate point sources along the circumference of the same polymeric particle. Consideration of these assumptions follows for a model with spherical geometry in a radiation source of cylindrical geometry.

In order for the recoil electrons from M to escape their respective point sources and interact with the lower density medium, the energy of the recoil electrons must be sufficiently high so that the probable path is many times longer than the point source proper. Using γ rays from a Co⁶⁰ source with an energy of 1.2 MeV, Compton scattering is produced with an average energy of 0.5 to 0.6 MeV. From depth dose charts for 0.5 MeV electrons in H₂O, such particles could interact at 1.5 to 2.0 mm.⁸ In material M with an electron density some six times greater, this depth would correspond to ca. 250–300 μm . Since the average point source of M has a radius of 2.5 μm , a penetration of 250 μm would be more than sufficient.

To substantiate assumption ii, the Compton scattering which is emanating from the particles of metal must traverse the second, third, and n th order nearest polymer neighbors, thereby overlapping $n - 1$ point sources in all directions radially. For each point source of metal considered, the scattering must cross several diameters of P and M. Again from the depth dose charts⁸ for 0.5 MeV electrons in H₂O, material P with essentially the same electron density as H₂O can penetrate 1500 to 2000 μm which corresponds to 1350 μm if successive diameters of P and M were lined up radially from the point source of interest. The corresponding domain overlap of 13 diameters of material P would be more than adequate.

To analyze assumption iii, a geometric construction is necessary. Such analysis (Appendix I) shows that the maximum distance which a recoil electron could travel within the immediate high electron density medium is $\sim 30 \mu\text{m}$. By recalling from assumption i that the penetration of secondary electrons in material M was 250 μm , the problem of nearest neighbor absorption can be neglected. Note that the contribution of 2δ is unimportant, since by inspection $2\delta < BC \ll 250 \mu\text{m}$.

(2) Derivation. The total value for chemical damage of a two-phase composite will equal the sum of its parts, or

$$\begin{aligned} G(-\text{units})_{\text{total}} &= (G_{P \rightarrow P}) + (G_{P \rightarrow M}) + (G_{M \rightarrow M}) + (G_{M \rightarrow P}) \\ &= (G_{P \rightarrow P}) + (G_{M \rightarrow P}) \end{aligned} \quad (1)$$

* Dental Research Center, University of North Carolina, Chapel Hill, N.C. 27514.

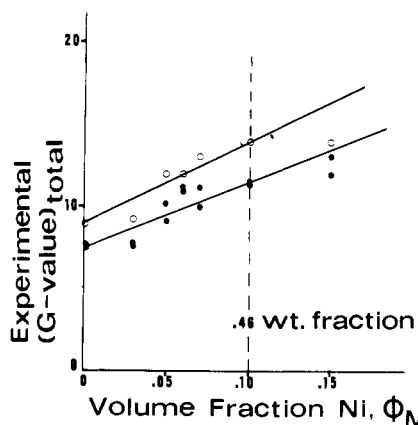


Figure 1. Influence of volume fraction of nickel on $(G - \text{value})_{\text{total}}$ for nylon-66/nickel-123 composites: (○) run 1; (●) runs 2 and 3. Dose = 64 Mrad.

where $G_{P \rightarrow P}$ represents the G value of P due to scattering which initially emanates from P particles, $G_{P \rightarrow M}$ represents the G value of M due to scattering which initially emanates from P particles, and so forth. The G value of material P as a result of self-absorption can be found readily from standard chemical analysis or from the depression of the melting point. The G values for terms 2 and 3 can be considered zero since the metallic phase does not undergo any permanent chemical change at these energy levels. The fourth term, the G value attributed to material P from the Coulombic interactions of metallic electrons, is the only unknown.

To find $(G - \text{value})_{\text{total}}$, the parameters ϕ_P , ϕ_M , θ_P , and θ_M are introduced. These are the volume fractions and the electron densities of P and M, respectively. For a composite, the total amount of electrons present equals

$$\theta_{\text{total}} = \phi_P \theta_P + \phi_M \theta_M \quad (2a)$$

recalling the identity $\phi_P + \phi_M = 1$

$$\theta_{\text{total}} = (1 - \phi_M) \theta_P + \phi_M \theta_M \quad (2b)$$

Material P through the addition of M becomes enriched with an increased number of secondary electrons (assumptions i-iii) equal to the final electron density divided by the initial electron density or,

$$\frac{\text{final electron density of the composite}}{\text{initial electron density of polymer}} = \frac{\theta_{\text{total}}}{\theta_P} \quad (3)$$

The increase in the apparent electron density of P suggests a dose:electron density equivalence for the case of a segregated distribution,

$$\left[\frac{G(-\text{units})_{\text{total}}}{(G_{P \rightarrow P})} \right] = \left(\frac{\theta_{\text{total}}}{\theta_P} \right) \quad (4)$$

Thus it follows that eq 4 expresses the $(G - \text{value})_{\text{total}}$ of a composite made up of a segregated distribution of material P and M.

To understand the contribution of $G_{P \rightarrow P}$ and $G_{M \rightarrow P}$, substitution of eq 2 into eq 4 and subsequent rearrangement is necessary.

$$G(-\text{units})_{\text{total}} = (G_{P \rightarrow P}) + \left[\phi_M \left(\frac{\theta_M}{\theta_P} - 1 \right) (G_{P \rightarrow P}) \right] \quad (5)$$

when $\theta_M \geq \theta_P$

By inspection of eq 5 with eq 1,

$$G_{M \rightarrow P} = \left[\phi_M \left(\frac{\theta_M}{\theta_P} - 1 \right) G_{P \rightarrow P} \right] \quad (6)$$

Note that when the electron densities are equivalent, $G(-\text{units})_{\text{total}} = (G_{P \rightarrow P})$.

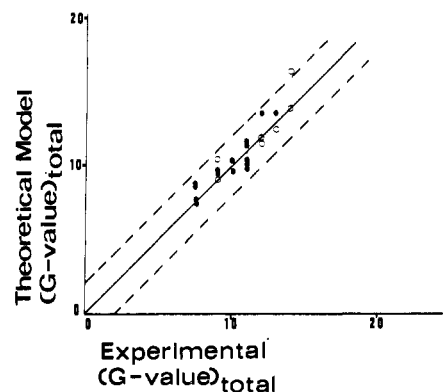


Figure 2. Comparison of $(G - \text{value})_{\text{total}}$ derived from theoretical considerations (e.g., eq 7) vs. experimental results (cf., Figure 1): (○) run 1; (●) runs 2 and 3. Dose = 64 Mrad.

In the present case, eq 5 can be solved for the low volume fraction of metal ($\phi_M < 0.15$). In previous work the $G(-\text{units})$ of nylon-66 determined by DTA equalled 9.0, 7.5, and 7.5 respectively for three successive runs.^{1,3} Substitution for $G_{P \rightarrow P}$ and for the theoretical electron densities of nylon (3.98×10^{23} electrons/cm³) and nickel (25.7×10^{23} electrons/cm³) yields,

$$G(-\text{units})_{\text{total}} = 9(1 + 5.46\phi_M) \quad (7)$$

(for run 1)

Similar equations can be derived for successive runs.

III. Results

The results obtained when the theoretical $(G - \text{value})_{\text{total}}$ (e.g., eq 7) is plotted against the experimental $(G - \text{value})_{\text{total}}$ (Figure 1) are illustrated in Figure 2. The solid line shows the 1:1 correlation while the dashed lines show the scatter envelope. The minimum $(G - \text{value})_{\text{total}}$ corresponds to the unmodified nylon material. Considering the problems associated with making representative segregated composites and the errors present in the measurement of the melting transition which affects the subsequent $(G - \text{value})_{\text{total}}$ calculation, the experimental data and the theoretical model show good correlation.

IV. Discussion

(1) Limitations and General Applicability. In the present work, a segregated distribution of nickel in nylon ($r_P/r_M \geq 5$) is used to compare the experimental $G(-\text{value})_{\text{total}}$ vs. the theoretical $G(-\text{value})_{\text{total}}$. If the assumptions are satisfied, the model may also apply to other geometries, material combinations, or multiple phases. For example, if a random distribution ($r_P/r_M \sim 1$) of a high and low electron density material is formed so that there is a high probability that secondary electrons can escape from high electron density medium and provide ionization and excitation to many particles of the low electron density material (assumption iii does not apply in this particular case), then the model would apply. In fact, the electron densities of the respective phases are unimportant save that in a two-phase system the higher electron density medium is designated θ_M , while the lower is designated θ_P . For a few light metals then, θ_P could represent a metallic phase and θ_M a polymer. This is to say nothing of the possibility of n -phase systems in which contributions from $n^2 G$ terms must be resolved to obtain $G(-\text{units})_{\text{total}}$.

To maintain a balanced perspective, it is important to consider factors which might restrict or limit the usefulness of a theory. One such parameter is the bulk geometry of the composite. In the nylon-nickel mixture tested, all specimens

were large (1.5 cm diameter \times 2 cm high) so that escape of secondary electrons at the free surface which results in a decreased number of Coulombic interactions was negligible. However, if the composite surface to volume ratio were increased, then the decreased interaction from secondary electrons could become more important. For sheets in which the thickness approaches the secondary electron range, surface effects would predominate.

As expressed in assumptions i–iii and eq 3, the purpose of the higher electron density medium is to provide additional secondary electrons to create more radiation damage in P. In the present segregated composites, each M particle is such an efficient secondary electron emitter that the electron density of P may be approximated by the total electron density. While the present analysis is limited to an ideal case, an accurate value of $G_{M \rightarrow P}$ might be possible when departures from ideality occur, if the total effective electron density or the overall secondary electron efficiency could be determined.

Whether or not an interaction may occur between phases is another concern. While eq 5 shows that $G(-\text{units})_{\text{total}} = (G_{P \rightarrow P})$ for the case in which $\theta_M = \theta_P$, more often than not interactions occur resulting in some form of deactivation or sensitization.^{9,10} In fact, phase interactions have been claimed for the case in which $\theta_M > \theta_P$, an indication that both a redistribution of absorbed energy and some form of deactivation or sensitization reaction is possible.¹¹ More data are needed to substantiate these findings, however.

Last, the model is only valid for a limited volume fraction of high electron density material, since an increase in M beyond a critical value yields no further benefits. This is the result of significant self-absorption of secondary electron ionization in M (a violation of assumption i) and/or significant absorption by an excessive number of neighboring M particles (a violation of assumptions ii and iii). In the present case studied, the limit might be inferred by the apparent deviation of Figure 1 at 15% loading of nickel by volume.

(2) Comparison with Previous Work. The present theoretical model and experimental data confirm and extend the previous work reported on polymeric systems in which an absence of electronic equilibrium exists.^{11–17} Several parallels may be drawn from the irradiation of a polymer sheet in contact with a metal sheet which are common with the current theory. Moreover, a few cases have been documented which corroborate the present observations that finely dispersed metals can increase the energy deposition in a lower electron density medium.

To a first approximation the absorbed energy near the surface of a thick polymer sheet which is in close proximity to a metal plate is analogous to the situation which exists throughout the segregated nylon–nickel composite. Substantiation of that statement is found from experimental data of Dutreix¹² which indicates that a 50–100% increase in energy absorption occurs near the partition boundary of carbon and metal ranging from $Z = 26$ to 82. The data indicated that a 50% increase in absorbed dose occurs for iron ($Z = 26$) or copper ($Z = 29$) vs. ca 65% in the present work for a high volume fraction of nickel ($\phi_M = 0.15$, $Z = 28$) in nylon. As the thickness of the polymer sheet between the metallic sheets decreases (from 5000 to 500 μm), Makhlis showed that superposition of the electron flux from opposite metallic screens tended to equalize the absorbed dose across the polymer thickness (cf. Figure 28, ref 11). This two-dimensional geometry is effectively extended to three dimensions in the present segregated composite design, since the small polymer particles (ca. 50 μm) are surrounded by a discontinuous envelope of metal. The result is a composite which exhibits distortion of electron equilibrium independent of thickness (providing the radiation can penetrate the bulk).

As eq 6 shows, the contribution to the $G(-\text{units})_{\text{total}}$ from

the metallic phase on the polymeric phase, i.e., a high electron density phase on a low electron density phase, is dependent upon the ratio (θ_M/θ_P). Verkhgradskii et al.¹³ substantiated that the absorbed dose in a thin polymer film (cellulose) may be increased if contacted with a material of higher Z . Using polymethyl methacrylate as a control contact material, gold ($\rho = 19.3 \text{ g/cm}^3$) increased the film's absorbed dose by 100% compared to glass ($\rho = 2.4 \text{ g/cm}^3$) which increased the polymer's absorbed dose by 10%. If lead, iron, and aluminum screens are compared, the mean absorbed energy in a thin polymer layer ($<5000 \mu\text{m}$) increases with Z , i.e., $\text{Pb} > \text{Fe} > \text{Al}$.¹¹ Finally, Spiers¹⁴ found that soft tissue received more radiation damage at the bone–tissue interface than at a distance more remote. Presumably, the ratio of electron densities contributed to the increased ionization received by the soft tissue which was in close proximity to the bone. Similarly, the effect was seen in the soft tissues which are contained in the Haversian systems of the bone. Dependent upon cavity geometry and radiation wavelength, the energy deposition increased by a factor of 3. This latter case is an excellent example of a biological three-dimensional mixture of finely divided phases having different electron densities in which interactions predominate.

In contrast to the irradiation of polymer films in contact with metal sheets, relatively little is known of the effects of radiation on polymer–metal mixtures. Gas evolution¹⁵ and cross-linking¹⁶ have been shown to increase with additions of powdered metals or metal compounds, the increased damage being attributed to "... an increase in the absorbed energy in the polymeric component because of [the ionizations of] secondary electrons generated by γ -irradiation in the metal".¹¹ It was not until Popova and Breger (1968)¹⁷ that the geometric parameters (number, size, shape) and absorbing capabilities of the powders were considered. The current experiments agree with the observations of these earlier investigators. Recognizing the assumptions and limitations of the model developed, the concepts described may provide further insight into these little-known composites.

V. Conclusions

From earlier gel and melting point measurements, evidence was presented which suggested that an increased absorption of energy resulted from the irradiation of nylon particles in a segregated distribution of nickel. In this paper, a model was presented to predict the effects which a higher electron density medium might have on a lower electron density medium under circumstances in which certain geometrical constraints were met. The theoretical $(G - \text{value})_{\text{total}}$ computed from this model agreed with the experimental $(G - \text{value})_{\text{total}}$ evaluated from the melting point data and Flory's equation. By an apparent increase in the total electron density of the nylon, an increase in the $G - \text{value}$ resulted. Clearly, a more efficient utilization of radiation energy could prove useful in a number of diverse applications.

Acknowledgment. This work was supported by The Division of Isotopes Development, U.S. Atomic Energy Commission.

Appendix I

Consider the structure of an ideal spherical composite. A particle of material P is drawn with particles of M aligned with their centers on the circumference of the P particle (cf. Figure 3). A geometrical construction is now made to determine the longest chord that can be inscribed within the torus which the metal particles sweep out. By inspection, the longest possible chord will deviate at its midpoint by the radius of the M particles. The error, δ , where the electron emerges from the imaginary torus when the particle has originated in the center

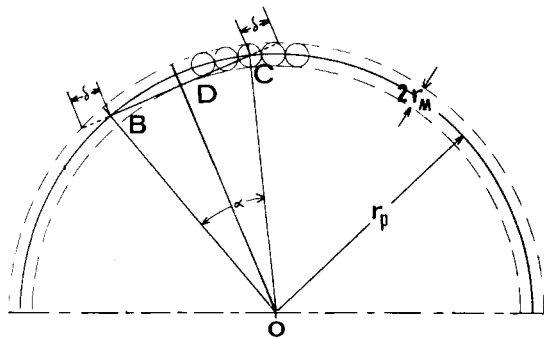


Figure 3. Schematic illustration of the geometry of high electron density particles along the circumference of a low electron density particle within a segregated network ($r_P/r_M \geq 5$).

of one of the immediate M particles, or the error, 2δ , when the particle has originated in the center of some neighboring n th particle not contained in the circumference of interest, will be much smaller than the chord length itself. Consequently, δ will be ignored in the first approximation. By defining the radius of material M, r_M , equal to $2.5 \mu\text{m}$ and the radius of material P, r_P , equal to $50 \mu\text{m}$, the longest chord that can be inscribed, \overline{BC} , equals,

$$\overline{BC} = 2r_P(\sin \frac{1}{2}\alpha) \quad (\text{i})$$

From the Pythagorean theorem,

$$\overline{b_O}^2 = \overline{OD}^2 + \overline{BD}^2 \quad (\text{ii})$$

Since $\overline{BD} = \frac{1}{2}\overline{BC}$, substitution of eq i into eq ii yields,

$$r_P^2 = (r_P - r_M)^2 + [r_P(\sin \frac{1}{2}\alpha)]^2 \quad (\text{iii})$$

Making numerical substitution for r_P and r_M gives $\alpha = 0.635$ rad Solving eq i for chord length, \overline{BC} , yields $31 \mu\text{m}$.

References and Notes

- (1) R. P. Kusy and D. T. Turner, *Macromolecules*, **4**, 266 (1971).
- (2) P. J. Flory, "Principles of Polymer Chemistry", Cornell University Press, Ithaca, N.Y., 1953, 568.
- (3) R. P. Kusy and D. T. Turner, *Macromolecules*, **4**, 337 (1971); *J. Polym. Sci., Part A-1*, **10**, 1745 (1972); *J. Polym. Sci.*, **12**, 2137 (1974); *Macromolecules*, **8**, 235 (1975).
- (4) J. Zimmerman, *J. Appl. Polym. Sci.*, **2**, 181 (1959).
- (5) A. Malliaris and D. T. Turner, *J. Appl. Phys.*, **42**, 614 (1971).
- (6) R. P. Kusy and D. T. Turner, *Nature (London)*, **229**, 58 (1971).
- (7) J. Gurland, "Plansee Proc.", F. Benesovsky, Ed., Springer, Vienna, 1962, p 507; *Trans. Metall. Soc. AIME*, **642** (1966).
- (8) G. R. White, "N.B.S. Report 1003" (1952), as cited by H. E. Johns and J. S. Laughlin, "Radiation Dosimetry", G. J. Hine and G. L. Brownell, Ed., Academic Press, New York, N.Y., 1956, p 50.
- (9) A. Charlesby, "Atomic Radiation and Polymers", Pergamon Press, London, 1960, pp 492-512.
- (10) A. Chapiro, "Radiation Chemistry of Polymeric Systems", Vol. XV, Interscience, New York, N.Y., 1962, pp 363 and 364.
- (11) F. A. Makhlis, "Radiation Physics and Chemistry of Polymers", Wiley, New York, N.Y., 1975, pp 103-105.
- (12) J. Dutreix, *Ann. Radiol.*, **7**, 233 (1964); *Radiobiol. Radioter.*, **4**, 12 (1963).
- (13) O. P. Verkhgradskii, et al., International Congress on Theoretical and Applied Chemistry, Moscow, July 1965, Report V-112 (Russian).
- (14) F. W. Spiers, *Br. J. Radiol.*, **22**, 521 (1949).
- (15) Yu. F. Nagornaya, "Radiatsionnaya Khimiya Polimerov", Moscow, "Nauka", 1966, p 354.
- (16) H. R. Anderson, U.S. Patent No. 3 098 808 (July 23, 1963).
- (17) L. V. Popova and A. Kh. Breger, All-Union Scientific Technical Conference on 20 Years of the Production and Application of Isotopes and Sources of Nuclear Radiation in the National Economy of the USSR. Section of Radiation Chemistry. Synopses of Reports, Atomizdat, 1968, p 55 (Russian).
- (18) For a "segregated" distribution, processing is carried out in such a way that the metallic particles reside only on the original surfaces of the polymeric particles, and the ratio of polymer to metal radii, (r_P/r_M), is large (≥ 5). While from a macroscopic viewpoint a random distribution results for all (r_P/r_M) since the particles used are quite small (r_P or $r_M < 150 \mu\text{m}$), only as $\lim (r_P/r_M) \rightarrow 1$ does a truly "random" distribution result at the microscopic level. This is the important distinction of a "segregated" distribution which, from a practical viewpoint, reduces by sixfold the volume fraction of metal necessary to achieve good electrical conductivity when (r_P/r_M) = 20^6 vs. ca. 1.7 .

Helix-Coil Stability Constants for the Naturally Occurring Amino Acids in Water. 11. Lysine Parameters from Random Poly(hydroxybutylglutamine-co-L-lysine)¹

M. K. Dygert,^{2a} G. T. Taylor,^{2b} F. Cardinaux, and H. A. Scheraga^{*2c}

Department of Chemistry, Cornell University, Ithaca, New York 14853.

Received January 26, 1976

ABSTRACT: The synthesis and characterization of water-soluble random copolymers containing L-lysine with N^5 -(4-hydroxybutyl)-L-glutamine, and the thermally induced helix-coil transitions of these copolymers in water, are described. The incorporation of L-lysine was found to decrease the helix content of the polymers at neutral pH. The Zimm-Bragg parameters σ and s for the helix-coil transition in poly(L-lysine) in water were deduced from an analysis of the melting curves in the manner described in earlier papers. The computed values of s indicate that, in the temperature range of 0-60 °C, lysine has a tendency to destabilize helical sequences, this tendency being minimal at ~25 °C and increasing at lower and higher temperatures.

Poly(L-lysine) has been studied extensively both in water and in aqueous salt solutions, and has been shown to exhibit the characteristics of random coil, α helix, or β structure depending on conditions of pH and temperature.³⁻⁹ The value of the standard free energy change, ΔG° , for conversion of an uncharged residue in the random coil state to an uncharged residue at the end of a preexisting α -helical region has been determined previously by application of the theory of Zimm and Rice¹⁰ to the analysis of titration data.¹¹⁻¹³ The temper-

ature dependence of this quantity, in turn, has provided a measure of ΔH° and ΔS° for this process. An independent measure of ΔH° obtained calorimetrically has verified these results.¹⁴ However, it has been assumed in these investigations that the helix-forming ability of an ionizable residue is independent of its state of ionization except for electrostatic repulsions between side chains when the residues are charged. Thus, the Zimm-Bragg helix stability constants,¹⁵ σ and s , obtained from these studies for an uncharged lysine residue